ADVANCED FUNCTIONAL MATERIALS
www.afm-journal.de

Facile Photo-Crosslinking of Azide-Containing Hole-Transporting Polymers for Highly Efficient, Solution-Processed, Multilayer Organic Light Emitting Devices

Junwoo Park, Changyeon Lee, Jihye Jung, Hyunbum Kang, Ki-Hyun Kim, Biwu Ma, and Bumjoon J. Kim**

A novel framework of azide containing photo-crosslinkable, conducting copolymer, that is, poly(azido-styrene)-random-poly(triphenylamine) (X-PTPA), is reported as a hole-transporting material for efficient solution-processed, multi-layer, organic light emitting diodes (OLEDs). A facile and energy-efficient crosslinking process is demonstrated with UV irradiation (254 nm, 2 mW/cm^2) at a short exposure time (5 min). By careful design of X-PTPA, in which 5 mol% of the photo-crosslinkable poly(azido-styrene) is copolymerized with hole-transporting poly(triphenylamine) (X-PTPA-5), the adverse effect of the crosslinking of azide moieties is prevented to maximize the performances of X-PTPA-5. Since the photo-crosslinking chemistry of azide molecules does not involve any photo-initiators, superior hole-transporting ability is achieved, producing efficient devices. To evaluate the performances of X-PTPA-5 as a hole-transporting/electron-blocking layer, Ir(ppy)$_3$-based, solution-processable OLEDs are fabricated. The results show high EQE (11.8%), luminous efficiency (43.7 cd/A), and power efficiency (10.4 lm/W), which represent about twofold enhancement over the control device without X-PTPA-5 film. Furthermore, micro-patterned OLEDs with the photo-crosslinkable X-PTPA-5 can be fabricated through standard photolithography. The versatility of this approach is also demonstrated by introducing the same azide moiety into other hole-transporting materials such as poly(carbazole) (X-PBC).

1. Introduction

To date, significant progress has been achieved in the area of organic light-emitting diodes (OLEDs) relative to their high performances through the multi-layer strategy based on the layer-by-layer vapor deposition.[1–6] However, many issues still remain as hurdles to cost-effective mass production of OLEDs, including poor utilization of materials, low fabrication yield, the need for expensive vacuum equipment, and high energy consumption during processing. To address these issues, OLED fabrications based on solution processes, such as spin-coating,[7–9] ink-jet printing,[10–12] and roll-to-roll printing,[13,14] have been developed, which provide fascinating alternative solutions for low-cost, large area OLEDs. However, desirable sequential-deposition without dissolution of the underlying layer (i.e., the orthogonal solvent method[15–18]) is required to fabricate high-performance, multi-layer-structured OLEDs by using the solution process. However, this is very challenging because the previously deposited layer could be dissolved by the solution of the subsequently deposited layer.

Two major routes have been developed to address this dissolution issue and fabricate the solution-processed, multi-layer structured OLEDs. One strategy involves thermal-crosslinkable materials, which can be solution processed and then transformed into an insoluble film by heat treatment.[19–30] For example, the hole-transporting copolymers that contain thermally reactive functional groups of benzocyclobutene and vinylbenzene can produce the solution-processable, multi-layer OLEDs that perform high efficiency.[19,20,22,25–30] However, most thermal cross-linking systems require a high annealing temperature (above 180 °C) and long processing times, ranging from 30 min to several hours, to obtain fully insoluble films, which could lead to the detrimental thermal degradation of the electroactive materials in the OLEDs.[31,32] Therefore, thermal crosslinking systems are generally limited to electroactive materials with high glass-transition temperatures. Also, the requirement of extensive thermal treatment can cause difficulty and inefficiency for mass production of the large-area devices. The other approach to producing the solution-processed, multi-layer structured OLEDs involves materials that contain photo-crosslinkable groups,[31,33–43] including oxetane,[35,37–39,41,42] acrylate,[31,34] and cinnamate.[31,36,40] Photo-crosslinking can be conducted at the much milder condition of

J. Park, C. Lee, J. Jung, H. Kang, K.-H. Kim, Prof. B. J. Kim
Department of Chemical and Biomolecular Engineering
Korea Advanced Institute of Science and Technology (KAIST)
Daejeon 305–701, Republic of Korea
E-mail: bumjoonkim@kaist.ac.kr
Prof. B. Ma
Department of Chemical and Biomedical Engineering
FAMU-FSU College of Engineering
Florida State University
Tallahassee, Florida, FL 32310, USA
E-mail: bma@fsu.edu

DOI: 10.1002/adfm.201401958

© 2014 WILEY-VCH Verlag GmbH & Co. KGaA, Weinheim

room temperature rather than thermal annealing. In addition, it has a great advantage in terms of processing freedom, that is, micro pixel patterns using the photolithography method.[31,37,43] However, less success has been achieved in applying the photo-crosslinking approach for solution processing of multi-layer OLEDs.[44,45] Because the process for the photo-crosslinking of currently available materials requires relatively long exposure to high-power UV irradiation, additional side reactions can occur during the crosslinking process, and they can have adverse effects on the efficiency and lifetime of the device. Also, both photo- and thermal-crosslinking approaches can potentially disturb the molecular packing, affecting both charge transport and device performance since a high loading of functional groups can interfere with molecular diffusion and the packing structure.[36,46] Therefore, although the photo-crosslinking concept is simple and powerful, the development of the cross-linkable materials with high efficiency for crosslinking with minimal disturbance in the electrical properties remains a great challenge.

Herein, we developed a novel platform of photo-crosslinkable azide (N_3)-containing, conducting polymers for use in highly efficient, solution-processed multi-layer OLEDs. Our system utilizes the small-sized, azide-functional moieties that can be photo-crosslinked at very low activation energy and fast reaction time without the use of a photoinitiator.[47,48] In order to explore the effect of azide-functional polymers on the device performance, we designed and synthesized hole-transporting poly(azido-styrene)-*random*-poly(triphenylamine) copolymers (X-PTPA) consisting of poly(triphenylamine) (PTPA) with small fractions (3–10 mol%) of poly(azido-styrene) (PS-N_3). The X-PTPA polymers can form insoluble, crosslinked films after UV irradiation for 5 min at extremely low UV power (2 mW/cm^2) with minimal disturbance on their molecular packing and hole mobility. Highly efficient, multi-layer OLEDs were fabricated with a crosslinked hole-transporting/electron-blocking layer (HTL/EBL) based on these polymers. The power efficiency of the device with the crosslinked film of X-PTPA polymer was increased dramatically by a factor of two in comparison to the control device without the X-PTPA film. Also, we expanded our platform to another azide-containing conducting polymers, i.e., poly(benzylcarbazole) (PBC), with a small fraction of PS-N_3 (poly(azido-styrene)-*random*-poly(benzylcarbazole) copolymer (X-PBC)), thereby demonstrating that our method is suitable for general use. Finally, in order to take full advantage of the photo-crosslinking approach, we fabricated pixelated OLEDs using the photo-crosslinkable X-PTPA film via the photolithography process.

2. Results and Discussion

To develop a new class of functional conjugated polymers as photo cross-linkable HTL/EBL, we designed a series of X-PTPA conducting random copolymers consisting of PTPA with different mole fractions (3–10 mol%) of PS-N_3. The PTPA conducting polymers, widely used as a hole-transporting material in OLEDs,[49–54] were selected based on their high hole-transporting ability and suitable energy levels (i.e., highest occupied molecular orbital (HOMO) and lowest unoccupied molecular orbital (LUMO)) that match up with those of PEDOT:PSS and emitting materials.[54] To increase the versatility of the azide functional groups for the use in other hole-transporting materials, we designed and synthesized polystyrene with a dangling N_3 substituent (PS-N_3) as a counter building block of PTPA and photo-crosslinkable group rather than using PTPA-N_3. Consequently, the photo-crosslinkable azide moiety could be easily applicable to other diverse conducting polymers simply by adding the PS-N_3 monomers during polymerization. It is worthwhile to note that low numbers of the mole fractions of PS-N_3 in the X-PTPA polymers (3–10 mol%) were targeted to avoid the adverse effect of crosslinked bridges on the molecular packing and to optimize the crosslinking behavior and the OLED device performance.

As shown in **Scheme 1**, the synthesis of X-PTPA starts from a simple one-pot polymerization of a mixture of 4-vinylbenzyl chloride (**1**) and *N*,*N*-diphenyl-4-vinylaniline (**2**) using a nitroxide-mediated radical-polymerization (NMP) initiator. To obtain the target copolymer of X-PTPA with different mole fractions of PS-N_3, we varied the molar ratio of **1**:**2** from 0:100 to 10:90 during the NMP polymerization. (The detailed synthesis of monomers **1**, **2**, **3** is described in the Supporting Information.) After the polymerization, the chlorine groups in the polymers were fully converted to azide groups by the nucleophilic substitution of chloride with sodium azide (NaN_3) in dimethylformamide. Residual NaN_3 was purified with a Soxhlet extractor using methanol, and, finally, X-PTPA polymers were obtained. The characteristics of the synthesized polymers, including the number-average molecular weight (M_n) and polydispersity index (PDI), are shown in **Table 1**. For convenience, these are labelled X-PTPA-3 (3 mol% PS-N_3), X-PTPA-5 (5 mol% PS-N_3), and X-PTPA-10 (10 mol% PS-N_3). To monitor the successful synthesis of X-PTPA, we performed Fourier transform infrared (FT-IR) and ^{1}H-nuclear magnetic resonance (NMR) measurements after every step of synthesis. In the FT-IR results in Figure S1 (Supporting Information), the distinct N_3 peak of X-PTPA is evident at 2100 cm^{-1},[47] whereas no peak was observed for the polymers before reaction with NaN_3.

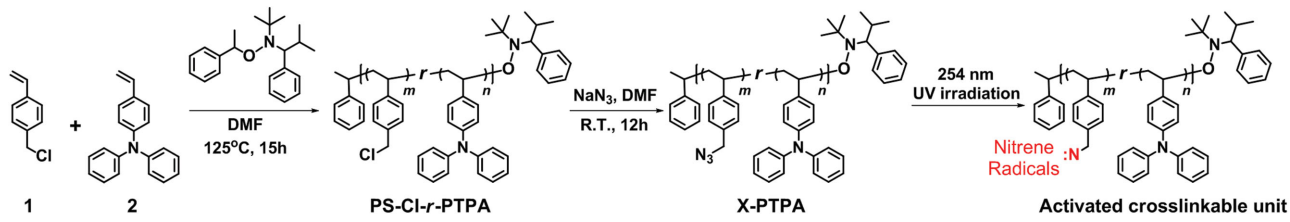

Scheme 1. Scheme for synthesis and photo-crosslinking reaction of X-PTPA polymers.

© 2014 WILEY-VCH Verlag GmbH & Co. KGaA, Weinheim

Table 1. Characteristics of photo-crosslinkable hole-transporting polymers used in this study.

	Polymer Information			Electrochemical Properties		
	Mole ratio of PS-N_3 : PTPA or PBC[a)]	M_n[b)] [kg/mol]	PDI[b)]	HOMO [eV]	LUMO [eV]	E_g^{opt} [eV]
				before[c)]/after[d)]	before/after	before[e)]/after[f)]
X-PTPA-3	3:97	20	1.38	–5.30/–5.31	–1.88/–1.88	3.42/3.43
X-PTPA-5	5:95	20	1.45	–5.30/–5.32	–1.88/–1.87	3.42/3.45
X-PTPA-10	10:90	20	1.42	–5.30/–5.32	–1.88/–1.87	3.42/3.45
X-PBC-5	5:95	20	1.56	–5.54/–5.55	–2.09/–2.14	3.45/3.41

[a)]The mole fractions of PS-N_3 in X-PTPA or X-PBC were measured based on the ratio of peak integrals from ^{1}H-NMR spectra; [b)]Measured from size exclusion chromatography (SEC) (calibrated with PS standards); [c,d)]The HOMO levels of polymer films before and after photo-crosslinking were measured by ultraviolet photoemission spectroscopy (UPS); [e,f)]The E_g^{opt} of polymer films before and after photo-crosslinking were determined based on the onset points of UV–Vis spectra.

In addition, the exact composition of PS-N_3 in X-PTPA was calculated from the NMR analysis in Figure S2 (Supporting Information). For example, the X-PTPA-5 polymers contained 5.05 mol% of PS-N_3, which corresponded almost exactly with mole fraction of 5 mol% that was initially desired.

To investigate the photo-crosslinking behavior and establish optimized crosslinking conditions, the X-PTPA-5 polymers were spun cast from chlorobenzene solution to afford a 30-nm-thick film on the glass substrate. The film was irradiated with a handheld UV lamp (254 nm wavelength) at very low power of 2 mW/cm^2. The photo-crosslinking step was conducted as a function of exposure time, which ranged from 0–5 min under an inert N_2 atmosphere. After the UV treatment, the crosslinked X-PTPA-5 film was immersed in a chlorobenzene solution and dried in a vacuum oven prior to the measurement. **Figure 1** shows the absorption spectra of the X-PTPA-5 films with different exposure times to the UV treatment. The as-spuncast X-PTPA-5 film (black line) indicated a strong absorption band from 310 to 350 nm, which was attributed mainly to the PTPA. The absorption spectrum of the X-PTPA-5 film with 5 min of UV irradiation was completely identical to that of the as-spun sample, and the result demonstrated that the exposure for 5 min was sufficient to provide complete solvent resistance for the film. However, partial dissolution occurred by solvent-rinsing in cases of 1–4 min samples, as evidenced by the gradual decrease in the absorbance intensity of the films compared to the as-spun sample. As shown in Figure S3 (Supporting Information), the thickness of the X-PTPA-5 film was unchanged after thorough rinsing by chlorobenzene when the PTPA-5 film was exposed to the UV irradiation longer than 5 min. In addition, the photo-crosslinking behavior of the X-PTPA-5 film was monitored by detecting the disappearance of the unique absorbance peak at 2100 cm^{-1} (Figure S4, Supporting Information), which agreed with the results of the UV absorption and film thickness measurements. Therefore, we determined that the crosslinking condition of 5 min of UV irradiation at 2 mW/cm^2 was optimal for fabricating insoluble X-PTPA-5 film. Then, we compared the surface morphologies of the film before and after the crosslinking process for 5 min. As described in the inset atomic force microscopy (AFM) topographic images (2 μm × 2 μm) of Figure 1, the root-mean-square (RMS) surface roughness did not change after photo-crosslinking, showing 0.23 and 0.22 nm with almost the same RMS values for the film before and after. This feature of mirror-like smoothness with extremely small RMS roughness (<1.0 nm) proved that photo-crosslinking of X-PTPA-5 films can be completed at the significantly mild condition of 5 min and 2 mW/cm^2 without any effect on the surface morphology, which is a notable advantage for the performance of multi-structure OLEDs.[27] In addition, the absorption spectra of the X-PTPA film before and after crosslinking indicated almost complete transparency in the visible spectrum between 400–700 nm, making the material suitable for use as an additional EBL on top of the ITO transparent electrode.

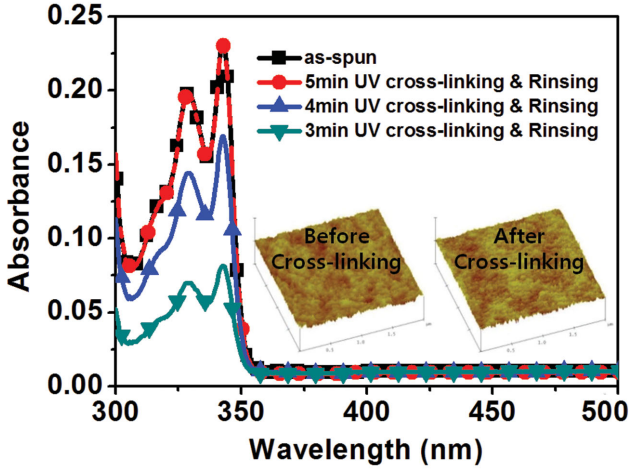

Figure 1. UV–Vis absorption spectrum of as-spun cast X-PTPA-5 thin film was compared to those of X-PTPA-5 after UV crosslinking at different exposure times and washed thoroughly by chlorobenzene. The inset figures compare the AFM topographic images of X-PTPA-5 thin films on the Si substrate before (left) and after (right) UV cross-linking.

In order to elucidate the relationship between photo-crosslinking and the electrochemical properties of the X-PTPA-5 polymers, ultraviolet photoemission spectroscopy (UPS), UV–Vis absorption spectroscopy, and space-charge-limited currents (SCLC) mobility measurements were conducted for the X-PTPA-5 films before and after the crosslinking process at optimized conditions of 5 min and 2 mW/cm^2. Table 1 compares the HOMO and LUMO levels as well as the optical bandgap value (E_g^{opt}). The HOMO levels of X-PTPA-5 films before and after the crosslinking process were determined to be –5.30 and –5.32 eV, respectively, by using UPS measurements. The LUMO levels of X-PTPA-5 films before and after the

© 2014 WILEY-VCH Verlag GmbH & Co. KGaA, Weinheim

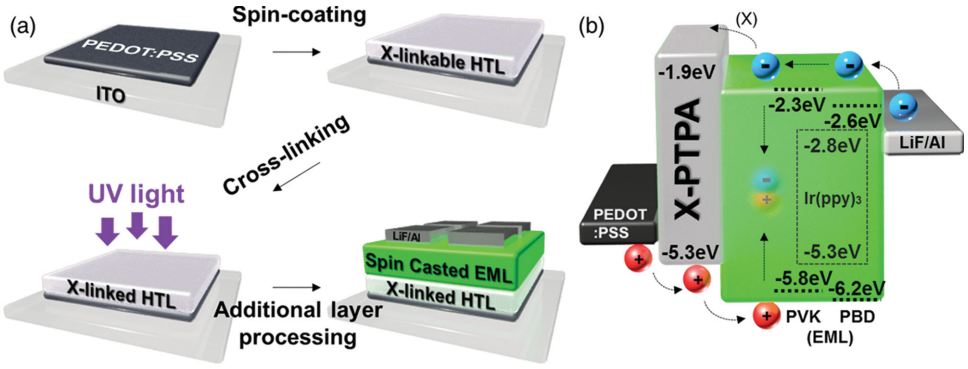

Scheme 2. a) OLED device structure with X-PTPA as cross-linkable HTL/EBL between PEDOT:PSS and spin-casted EML; b) Energy diagram of various materials used in this study.

crosslinking process were determined to be –1.88 and –1.87 eV, respectively, from the HOMO level and the E_g^{opt} value. Therefore, the HOMO, LUMO levels and E_g^{opt} values were almost the same at before and after the crosslinking within the error range of the measurements. Also, the hole mobilities of the X-PTPA-5 films before and after the crosslinking process (5 min and 2 mW/cm^2) were measured using the SCLC method.[55–58] The hole mobility values of the X-PTPA-5 films with different film thicknesses are summarized in Table S1 (Supporting Information). It is remarkable that the hole mobilities of the X-PTPA-5 polymers were almost unchanged by the crosslinking process under the optimized condition. Thus, it can be concluded that the electrochemical, electrical, and optical properties of the crosslinked X-PTPA-5 film were not affected by the crosslinking process, demonstrating the advantage of our azide molecule platform.

The hole-transporting and electron-blocking properties of the X-PTPA-5 films were then evaluated by introducing them into solution-processable, multi-layered OLEDs. **Scheme 2**a illustrates the details of the fabrication of the OLED devices with X-PTPA-5 HTL/EBL. X-PTPA-5 film was deposited on the indium tin oxide (ITO)/poly(3,4-ethylenedioxythiophene):poly (styrene sulfonate) (PEDOT:PSS) film using spincoating from the chlorobenzene solution and then cross-linked by irradiation with UV light. Then, the blending solution of poly(9-vinylcarbazole) (PVK), 2-(4-biphenylyl)-5-phenyl-1,3,4-oxadiazole (PBD) and tris[2-phenylpyridinato-C^2,N]iridium(III) (Ir(ppy)$_3$) was stacked on the crosslinked X-PTPA-5 HTL/EBL to form the emitting layer (EML), and the fabrication of the OLED device was completed by depositing the LiF/Al electrode. Thus, we utilized the simple, yet efficient, device configuration of ITO/PEDOT:PSS/X-PTPA-5/PVK:PBD:Ir(ppy)$_3$/LiF/Al in order to determine the effectiveness of the X-PTPA-5 film on the device performance.[59,60] Scheme 2b shows the structures of the fabricated device and the energy levels of each component. In particular, the proper HOMO level (–5.3 eV) of the X-PTPA-5 layer is located between the PEDOT:PSS film and the PVK:PBD:Ir(ppy)$_3$ EML, which is suitable for decreasing the hole-injection barrier in the OLED device. Also, the high LUMO level (–1.9 eV) of the X-PTPA-5 film can reduce the leakage current by blocking electron injection from the cathode. **Figure 2**a compares the normalized electroluminescence (EL) of the devices with and without the X-PTPA-5 film. Both the control and X-PTPA-5 devices involved pure green-emission spectra from the Ir(ppy)$_3$ dopant. To establish the optimal condition for the device operation with the X-PTPA-5 HTL/EBL, we fabricated several sets of devices with various UV exposure times. Figure 2b shows the trends of the external quantum efficiency (EQE) values in various devices as a function of UV-irradiation times, ranging from 3 to 20 min. All devices had an initial deposition of a 30-nm thick X-PTPA-5 layer prior to UV-irradiation and subsequent deposition of EML. The EQE values were enhanced remarkably with the use of X-PTPA-5 HTL/EBL. For example, with 5 min of UV irradiation, the X-PTPA-5 device showed a greatly improved EQE value of 11.8%, as opposed to only 6.2% for the control device without the X-PTPA-5 film. Also, it was observed that the control of the photo-crosslinking condition was important to optimize the OLED performance. For example, Figure 2b shows that 5 min of UV-irradiation at a power of 2 mW/cm^2 was the optimal condition. The performance of the OLED with the shorter UV-irradiation time (2–4 min) had reduced EQE values compared to that of the optimal device, although their values were still higher than that

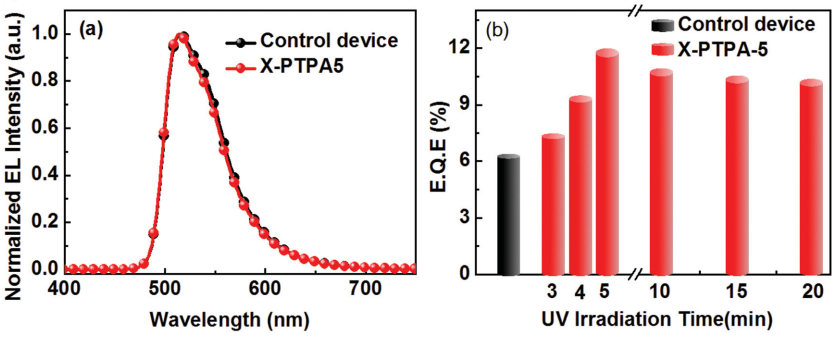

Figure 2. a) Characteristics of the normalized EL spectra of the control and X-PTPA-5 phosphorescent device at the current density of 100 mA/cm^2; b) EQE values of the X-PTPA-5 devices with different UV irradiation times ranging from 3 to 20 min; All devices had an initial deposition of 30-nm thick X-PTPA-5 layer prior to UV exposure and subsequent deposition of emitting layer.

© 2014 WILEY-VCH Verlag GmbH & Co. KGaA, Weinheim

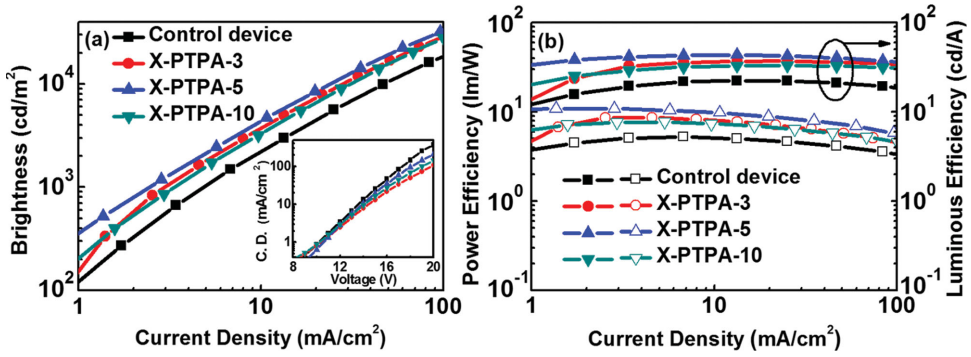

Figure 3. a) Brightness–current density and current density–voltage (inset); b) Power efficiency–current density (open symbols) and luminous efficiency–current density (filled symbols) for control and X-PTPA-3, X-PTPA-5, and X-PTPA-10 OLED devices.

of the control device without the X-PTPA-5 film. It is suggested that, as indicated by the photo-crosslinking study in Figure 1, the shorter UV irradiation time was not sufficient to produce complete crosslinking of the X-PTPA-5 films, which led to partial dissolution of the film during the spin coating of the EML solution. And, the longer UV irradiation time (>10 min) also resulted in slightly decreased EQE values, ranging from 11.8 to 10.3%. This result might be due to the formation of more than required crosslinking bridges in the X-PTPA-5 film that can disturb the molecular packing between X-PTPA-5 polymers, thus decreasing the charge transport ability.[36,46] However, we noted that once the X-PTPA-5 became fully crosslinked (after 5 min UV-irradiation), the X-PTPA-5 devices had much higher EQE values, regardless of the crosslinking time, than that of the control device.

The other characteristics of the devices with and without X-PTPA-5 HTL/EBL were measured by using the optimal conditions shown in **Figure 3**. **Table 2** provides a summary of the device characteristics of the X-PTPA-5 devices. The current densities of the X-PTPA-5 device as a function of driving voltages were slightly lower than that of the control device (Figure 3a). However, the device's other performances including EQE, turn-on voltage, brightness, power and luminous efficiencies were enhanced dramatically. The turn-on voltage of the X-PTPA-5 device was 6 V at 0.1 cd/m^2, which was lower than that (7 V) of the control device. This reduced operational voltage was attributed to the decreased hole-injection barrier from the appropriate HOMO energy level of X-PTPA-5.[27,28,61] And the maximum brightness was significantly increased from the 42 400 cd/m^2 recorded for the control device to 52 600 cd/m^2 for the X-PTPA-5 device. More importantly, the X-PTPA-5 device showed about a twofold enhancement of the maximum EQE (11.8%), the luminous efficiency (43.7 cd/A) and the power efficiency (10.4 lm/W) over the control device, which had values of 6.2%, 22.3 cd/m^2, and 5.2 lm/W, respectively.

To gain a deeper insight into the performances of the X-PTPA device, we developed a series of X-PTPA polymers with different azide mole fractions including X-PTPA-3, X-PTPA-5, and X-PTPA-10, and we explored their effects on the OLED device performance. Controlling the mole fraction of the photo-crosslinking moiety is very important in order to optimize the device performance. For instance, it is suggested that, as the amounts of the azide groups in X-PTPA polymer increase, the UV irradiation time required for fully crosslinking is reduced significantly. However, the device performances could be influenced adversely by the reduced amount of the conducting PTPA moiety and the presence of heavily introduced, cross-linking bridges in conjugated polymers that often disturb their molecular packing. In contrast, as the amount of the azide groups decreased, the adverse effect of the crosslinking bridges on the charge transport in the film was minimized. However, the X-PTPA polymers require much longer UV irradiation time to be perfectly crosslinked, which could lead to the potential photo-degradation of the conjugated polymers.[36] In these regards, we varied the mole fraction of PS-N_3 in X-PTPA as 3, 5, and 10 mol% (X-PTPA-3, X-PTPA-5, and X-PTPA-10) (Table 1). (Detailed procedures for the synthesis of X-PTPA-3 and X-PTPA-10 polymers are provided in the Supporting Information.) As used for the previous crosslinking study for X-PTPA-5 polymer, the crosslinking tests for X-PTPA-3, X-PTPA-5, and X-PTPA-10 were performed with 254 nm UV irradiation at the power of 2 mW/cm^2 (Figure S5, Supporting Information).

Table 2. Performances of the control and X-PTPA and X-PBC OLED devices.

	Control device[a)]	X-PTPA-3	X-PTPA-5	X-PTPA-10	X-PBC-5
Turn-on voltage [V][b)]	7	6	6	6	6
max. brightness [cd/m^2]	42 400	46 200	52 600	50 700	50 600
max. EQE [%]	6.2	10.1	11.8	9.0	9.0
max. current efficiency [cd/A]	22.3	37.2	43.7	33.2	33.2
max. power efficiency [lm/W]	5.2	8.7	10.4	7.7	7.6

[a)]The device had no layer of X-PTPA or X-PBC; [b)]Turn-on voltage at 0.1 cd/m^2.

© 2014 WILEY-VCH Verlag GmbH & Co. KGaA, Weinheim

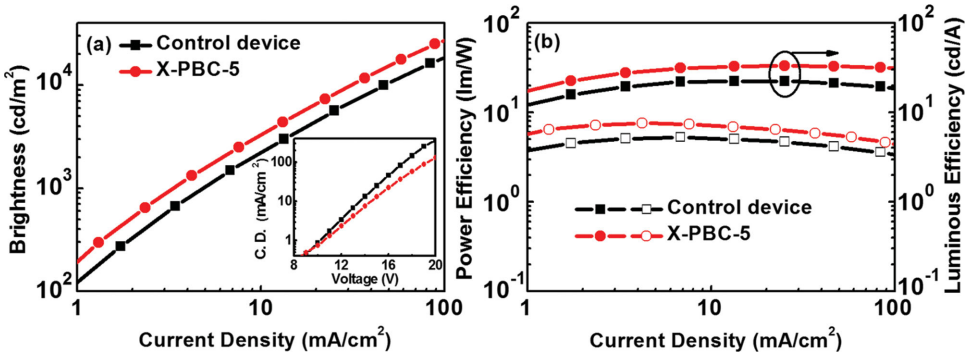

Figure 4. a) Brightness–current density and current density-voltage (inset); b) Power efficiency–current density (open symbols) and luminous efficiency–current density (filled symbols) for control and X-PBC-5 OLED device.

X-PTPA-10 showed the fastest UV-irradiation time of 4 min in contrast to 5 min for X-PTPA-5 and 8 min for X-PTPA-3. By using the above crosslinking conditions for each polymer, X-PTPA-3, X-PTPA-5, and X-PTPA-10 were used as HTL/EBL of OLEDs, and the device performances were evaluated. The results are summarized in Figure 3 and Table 2. The profiles of current density as a function of driving voltages showed that all of the X-PTPA devices had slightly lower current densities than that of the control device in Figure 3a. And the turn-on voltages for all of the X-PTPA devices were the same (6 V at 0.1 cd/m^2), which was lower than that of the control device (7 V). These features were consistent with the previous result observed for the X-PTPA-5 device. The optimized conditions with various UV-irradiation times were constructed by fabricating and measuring various sets of devices (Figure S6). Interestingly, compared to the optimal crosslinking time (5 min) observed for the X-PTPA-5 device, the X-PTPA-10 and X-PTPA-3 devices had different optimal crosslinking times of 4 and 8 min, respectively, for producing the highest EQE values in the OLED devices, which agreed well with the numbers required for the complete crosslinking. However, at the optimal crosslinking conditions, both the X-PTPA-10 and X-PTPA-3 devices showed slightly lower EQE values of 9.0 and 10.1% compared to that of the X-PTPA-5 device. Although the X-PTPA-10 polymer can be crosslinked with shorter process time due to the presence of the increased PS-N_3 mole fraction, the excess of PS-N_3 groups reduced the relative amount of the conducting PTPA moiety and produced more crosslinking bridges than were needed for producing insoluble film, which could disrupt the molecular packing of the conjugated polymers and the current density in the X-PTPA-10 device. As a result, Figure 3b shows that the power and luminous efficiencies of X-PTPA-10 were less than those of X-PTPA-3 and X-PTPA-5 mainly due to the decrease in the charge transport property. Therefore, we determined that X-PTPA-5 had the device efficiency. However, we noted that all of the characteristics of the X-PTPA devices, including their EQE, maximum brightness, power, and luminous efficiencies, were enhanced significantly compared to the control device, regardless of their PS-N_3 mole fractions (3–10%).

To examine the possibility for the general use of our azide-containing copolymer system, we applied the photo-crosslinkable platform of PS-N_3 to another type of random copolymer that consisted of hole transporting poly(vinyl benzyl carbazole) with 5% PS-N_3 (X-PBC-5). It was observed that the X-PBC-5 film could be photo-crossslinked to produce insoluble film upon UV irradiation for 5 min at the UV power of 2 mW/cm^2, which is the same condition determined for the X-PTPA-5 polymers. Also, neither the electrochemical nor the optical properties of the X-PBC-5 film were not affected by the crosslinking process and these properties are summarized in Table 1. Then, we fabricated the solution processed OLEDs by using X-PBC-5 as an HTL/EBL with the device configuration of ITO/PEDOT:PSS/X-PBC-5/PVK:PBD:Ir(ppy)$_3$/LiF/Al (Scheme S1). As shown in **Figure 4** and Table 2, the performances of the X-PBC device were improved remarkably to an extent that was analogous to that of the X-PTPA-5 device. Compared to the control device, the turn-on voltage of the X-PBC-5 device was reduced to 6 V, and the EQE value, the current, and power efficiencies were enhanced up to 9.0%, 33.2 cd/A, and 7.6 lm/W, respectively. The enhancement trends in the performances of the X-PBC-5 device were in good agreement with those of the X-PTPA HTL/EBL device. Thus, we consider that our photo-crosslinkable azide platform can be expanded to diverse conducting polymers through simple copolymerization of the conducting polymer and PS-N_3.

Another crucial advantage of these photo-crosslinkable azide-containing polymers is the feasibility of micrometer-scale pixelation for display applications via photolithography. The process for photolithography is illustrated in the inset of **Figure 5**a. The X-PTPA-5 was spin-coated from chlorobenzene solution onto the PEDOT:PSS/Si substrate, and then photo-crosslinking with 5 min of UV irradiation at 2 mW/cm^2 was conducted by covering the film with a photo-lithographic mask to produce a mask pattern on the X-PTPA-5 film. We just used TEM grid with each mesh of the 37 μm × 37 μm dimensions as a pattern mask for simple demonstration of the photolithographic process. Then, the film was washed several times with chlorobenzene to selectively remove the uncrosslinked X-PTPA-5 film, producing the square dot patterns (Figure 5a). To exploit the micro-patterned X-PTPA-5 HTL/EBL for pixelated OLEDs, a green light-emitting OLED device was fabricated with the same configuration as discussed above but with the patterned X-PTPA-5 film. The blending solution of PVK:PBD:Ir(ppy)$_3$ was stacked on the micro-patterned X-PTPA-5 film to form the EML, and then

© 2014 WILEY-VCH Verlag GmbH & Co. KGaA, Weinheim

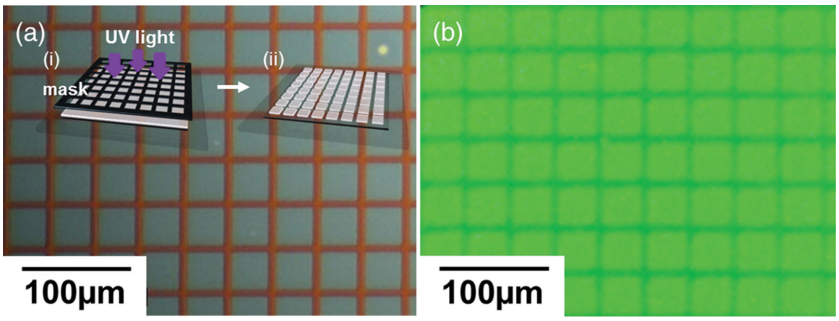

Figure 5. The inset of (a) shows the illustration of process for photolithography: i) crosslinking (254 nm UV; 2 mW/cm^2) with mask; ii) developing (with chlorobenzene). a) Optical microscopy image of X-PTPA-5 patterns (37 μm × 37 μm squares, 42-μm pitch and 5-μm bar width) on a Si substrate under UV lamp illumination; b) Photograph of micro-pixel patterned OLED device under operation (2 mA): 37-μm square-width pixels in OLEDs emitting much stronger green light due to the presence of X-PTPA-5 film.

the LiF/Al electrode was sequentially deposited. Figure 5b shows an optical microscope image of the green-emitting OLEDs under operation. The apparent difference in the brightness of the light was evident between the square-patterned dots (with X-PTPA-5 HTL/EBL) and the surrounding cross-lined patterns (without X-PTPA-5 HTL/EBL). In addition, the device performances of the micro-pixelated region and the non-pixelated region were compared as summarized in Table S2 (Supporting Information), and a clear contrast of the device performances was evident between the two different regions. Therefore, we proved that our system is beneficial for fabricating pixelated OLEDs via the simple photolithography process.

3. Conclusions

In this study, we demonstrated highly efficient, solution-processed OLEDs using X-PTPA-5 as photo-crosslinkable HTL/EBL, which could be processed by an extremely fast process with minimal UV energy. The X-PTPA-5 device showed greatly improved maximum EQE (11.8%), luminous efficiency (43.7 cd/A) and the power efficiency (10.4 lm/W), a twofold enhancements over the control device. Therefore, it is evident that the X-PTPA-5 HTL/EBL would be beneficial for use in solution-processed, multi-layer structured OLEDs by enhancing better electron and hole balance and blocking electron leakage. Furthermore, the micro-pixel patterning by the photo-crosslinkable X-PTPA-5 can be fabricated through a simple, fast process of photolithography, and the pixelated multi-layer OLEDs with X-PTPA-5 can be achieved with stable device operation. The X-PTPA-5 polymers enabled the facile photo-crosslinking process with high resolution and low energy consumption, making them suitable for large-area and flexible-light source applications. Furthermore, the versatility of our photo-crosslinkable molecular platform was significantly increased by expanding its use into X-PBC-5 polymers, thus providing significant potential for use in various types of hole/electron transporting and emitting conjugated polymers in the OLEDs and even the other conjugated polymers for various organic electronics.[62,63]

4. Experimental Section

Synthesis: The detailed syntheses of the monomers and the NMP initiator are shown in the Supporting Information.

Poly(azido-styrene)-random-Poly(triphenylamine) Copolymer (X-PTPA): First, the poly(4-chloromethyl styrene)-*random*-poly(triphenylamine) copolymers (PS-Cl-*r*-PTPA) were co-polymerized using *N*,*N*-diphenyl-4-vinylaniline (**2**) with 3, 5, and 10 mol% of 4-vinylbenzyl chloride (**1**) via in situ nitroxide-mediated radical polymerization under an N_2 atmosphere in anhydrous DMF at 125 °C. Then, the photo-crosslinkable X-PTPA (Scheme 1) was readily obtained from the PS-Cl-*r*-PTPA polymer via the nucleophilic substitution of chlorine atoms with 1.2 equiv. of NaN_3 in DMF at the ambient condition for 12 h. The polymers were precipitated with methanol and the resulting precipitates were then filtered. Residual NaN_3 was removed by Soxhlet extraction with methanol for 8 h.

Poly(azido-styrene)-random-Poly(benzylcarbazole) Copolymer (X-PBC): The same procedure described above was applied to the X-PBC-5 polymer (Scheme S1 in Supporting Information).

Characterizations: All ^{1}H-NMR spectra were recorded at 400 MHz using $CDCl_3$ as a solvent at room temperature. The chemical shifts of all ^{1}H-NMR spectra are referenced to the residual signal of $CDCl_3$ (δ 7.26 ppm) by an Agilent 400-MHz, 54-mm NMR DD2 instrument. The mole fraction of PS-N_3 in polymers were measured based on the ratio of integrals between the azidomethyl (N_3-C$\underline{H}_2$-) peaks around 4.05 ppm and aromatic peaks (6.4–7.2 ppm) from ^{1}H-NMR spectra (Table 1). FT-IR measurements were obtained using Alpha FT-IR spectrometer (Bruker Optics). The UV–Vis absorption spectra were obtained using a UV-1800 spectrophotometer (Shimadzu Scientific Instruments) at room temperature. The thin films were prepared by spin coating a chlorobenzene solution of polymers at 3000 rpm for 40 s onto a glass substrate. The E_g^{opt} value of polymer films was determined based on the onset points of the UV–Vis spectra. The M_n and PDI values of the polymers were measured using a SEC system (Waters 2414) equipped with UV and RI detectors, which were calibrated by PS standards with tetrahydrofuran as an eluent at room temperature. The HOMO levels of polymer films before and after photo-crosslinking were obtained by UPS measurements (ESCA 2000 Sigma Probe, VG Scientific) using a He I (21.22 eV) source. The samples were prepared by spin coating from the chlorobenzene solution of polymers onto Si substrate. The thin films were prepared in a N_2-filled glove box and immediately transferred to the UPS chamber, which was maintained at an ultra-high vacuum of 1 × 10^{-10} Torr. The HOMO energy levels of the polymer films were determined using the following equation:

$$\mathrm{HOMO} = h\nu - \left| E_{\mathrm{cutoff}} - \mathrm{HOMO}_{\mathrm{onset}} \right|$$

where: $h\nu$ is 21.22 eV as the He I source; E_{cutoff} is the high binding energy cutoff from the vacuum level; and $HOMO_{onset}$ is the low binding energy cut off from the sample.

Device Fabrication and Measurements: To evaluate the performances of X-PTPA-3, X-PTPA-5, X-PTPA-10, and X-PBC-5 as photo-crosslinkable HTL/EBL, solution-processable phosphorescent OLEDs were fabricated with the following structures: ITO/PEDOT:PSS/crosslinked X-PTPA-3, X-PTPA-5, X-PTPA-10, or X-PBC-5/PVK:Ir(ppy)$_3$:PBD/LiF/Al. The PVK, PBD and Ir(ppy)$_3$, which were purchased from Sigma Aldrich, were used without further purification. ITO-coated glass substrates were subjected to ultrasonication in acetone and 2% Helmanex soap in water, followed by extensive rinsing with ultrasonication in deionized water and then in isopropyl alcohol. After precleaning, the substrates were dried in an oven at 80 °C for 2 h. PEDOT:PSS (Clevios P VP AI4083) solution was spin-coated onto O_2-plasma treated ITO substrates at 4000 rpm for

© 2014 WILEY-VCH Verlag GmbH & Co. KGaA, Weinheim

40 s. Then, the PEDOT:PSS film was baked at 150 °C for 20 min in air to remove the residual water in the film. The substrates were transferred to a glove box immediately, and the following procedures were performed in inert conditions. Photo-crosslinkable X-PTPA-3, X-PTPA-5, X-PTPA-10, or X-PBC-5 was deposited onto the PEDOT:PSS films by spin coating at 3000 rpm for 40 s. Then, the films were crosslinked under 254 nm UV-irradiation for different exposure times (0–20 min) by using a handheld UV irradiator (2 mW/cm^2). For deposition of EML, a blend solution of PVK:PBD:Ir(ppy)$_3$ ((70:30):2.4 w/w) was dissolved in chlorobenzene and stirred at 80 °C for 24 h. After filtering the blend solution using a 0.2-μm poly(tetrafluoroethylene) (PTPE) syringe filter, the solution was spin-coated onto the crosslinked X-PTPA-3, X-PTPA-5, X-PTPA-10, or X-PBC-5 film at 2000 rpm for 40 s. Then, the HTL film on the substrate was annealed at 100 °C for 30 min to remove any residual chlorobenzene solvent. The substrates were then placed in an evaporation chamber and held under a high vacuum (<10^{-6} Torr) for more than 1 h before evaporating ≈1 nm of LiF/100 nm of Al. The configuration of the shadow mask afforded four independent devices on each substrate. We measured the performances and the EL characteristics of the devices using a current and voltage source meter (Keithley 2400) and a spectroradiometer (Minolta, CS-2000).

Supporting Information

Supporting Information is available from the Wiley Online Library or from the author.

Acknowledgements

This research was supported by the National Research Foundation Grant (2012M1A2A2671746), and by the Global Frontier R&D Program on Center for Multiscale Energy System (2012M3A6A7055540), funded by the Korean Government. This research was also supported by the New & Renewable Energy Core Technology Program of KETEP Grant (2011-T100100587), funded by the Ministry of Trade, Industry & Energy, Republic of Korea. Authors also acknowledge the KAIST-KUSTAR Research Project and Samsung Display Co. for the financial support. B. Ma thanks Florida State University for the startup fund support through the University Energy & Materials Initiative.

Received: June 14, 2014
Revised: August 19, 2014
Published online: October 13, 2014

[1] C. W. Tang, S. A. VanSlyke, *Appl. Phys. Lett.* **1987**, *51*, 913.
[2] J. R. Sheats, *Science* **1997**, *277*, 191.
[3] R. H. Friend, R. W. Gymer, A. B. Holmes, J. H. Burroughes, R. N. Marks, C. Taliani, D. D. C. Bradley, D. A. Dos Santos, J. L. Bredas, M. Logdlund, W. R. Salaneck, *Nature* **1999**, *397*, 121.
[4] B. W. D'Andrade, S. R. Forrest, *Adv. Mater.* **2004**, *16*, 1585.
[5] H. Sasabe, J. Kido, *Chem. Mater.* **2010**, *23*, 621.
[6] C. A. Zuniga, S. Barlow, S. R. Marder, *Chem. Mater.* **2010**, *23*, 658.
[7] J. P. J. Markham, S. C. Lo, S. W. Magennis, P. L. Burn, I. D. W. Samuel, *Appl. Phys. Lett.* **2002**, *80*, 2645.
[8] F. Huang, Y.-J. Cheng, Y. Zhang, M. S. Liu, A. K. Y. Jen, *J. Mater. Chem.* **2008**, *18*, 4495.
[9] C. Lee, D. J. Kang, H. Kang, T. Kim, J. Park, J. Lee, S. Yoo, B. J. Kim, *Adv. Ener. Mater.* **2014**, *4*, 1301345.
[10] T. R. Hebner, C. C. Wu, D. Marcy, M. H. Lu, J. C. Sturm, *Appl. Phys. Lett.* **1998**, *72*, 519.
[11] J. Bharathan, Y. Yang, *Appl. Phys. Lett.* **1998**, *72*, 2660.
[12] S.-C. Chang, J. Liu, J. Bharathan, Y. Yang, J. Onohara, J. Kido, *Adv. Mater.* **1999**, *11*, 734.
[13] R. R. Søndergaard, M. Hösel, F. C. Krebs, *J. Polym. Sci. B: Polym. Phys.* **2013**, *51*, 16.
[14] A. R. Cho, E. H. Kim, S. Y. Park, L. S. Park, *Synth. Met.* **2014**, *193*, 77.
[15] H. Wu, F. Huang, Y. Mo, W. Yang, D. Wang, J. Peng, Y. Cao, *Adv. Mater.* **2004**, *16*, 1826.
[16] X. Gong, S. Wang, D. Moses, G. C. Bazan, A. J. Heeger, *Adv. Mater.* **2005**, *17*, 2053.
[17] T. Earmme, S. A. Jenekhe, *Adv. Funct. Mater.* **2012**, *22*, 5126.
[18] S. Ohisa, G. Matsuba, N. L. Yamada, Y.-J. Pu, H. Sasabe, J. Kido, *Adv. Mater. Interfaces* **2014**, DOI: 10.1002/admi.201400097.
[19] G. Klaerner, J. I. Lee, V. Y. Lee, E. Chan, J. P. Chen, A. Nelson, D. Markiewicz, R. Siemens, J. C. Scott, R. D. Miller, *Chem. Mater.* **1999**, *11*, 1800.
[20] S. Dailey, W. J. Feast, R. J. Peace, I. C. Sage, S. Till, E. L. Wood, *J. Mater. Chem.* **2001**, *11*, 2238.
[21] X. Z. Jiang, S. Liu, M. S. Liu, P. Herguth, A. K. Y. Jen, H. Fong, M. Sarikaya, *Adv. Funct. Mater.* **2002**, *12*, 745.
[22] L. D. Bozano, K. R. Carter, V. Y. Lee, R. D. Miller, R. DiPietro, J. C. Scott, *J. Appl. Phys.* **2003**, *94*, 3061.
[23] B. Lim, J.-T. Hwang, J. Y. Kim, J. Ghim, D. Vak, Y.-Y. Noh, S.-H. Lee, K. Lee, A. J. Heeger, D.-Y. Kim, *Org. Lett.* **2006**, *8*, 4703.
[24] Y.-H. Niu, M. S. Liu, J.-W. Ka, A. K. -Y. Jen, *Appl. Phys. Lett.* **2006**, *88*, 093505.
[25] G. K. Paul, J. Mwaura, A. A. Argun, P. Taranekar, J. R. Reynolds, *Macromolecules* **2006**, *39*, 7789.
[26] Y. H. Niu, M. S. Liu, J. W. Ka, J. Bardeker, M. T. Zin, R. Schofield, Y. Chi, A. K. Y. Jen, *Adv. Mater.* **2007**, *19*, 300.
[27] B. Ma, F. Lauterwasser, L. Deng, C. S. Zonte, B. J. Kim, J. M. J. Frechet, C. Borek, M. E. Thompson, *Chem. Mater.* **2007**, *19*, 4827.
[28] B. Ma, B. J. Kim, D. A. Poulsen, S. J. Pastine, J. M. J. Frechet, *Adv. Funct. Mater.* **2009**, *19*, 1024.
[29] C. A. Zuniga, J. Abdallah, W. Haske, Y. D. Zhang, I. Coropceanu, S. Barlow, B. Kippelen, S. R. Marder, *Adv. Mater.* **2013**, *25*, 1739.
[30] N. Aizawa, Y.-J. Pu, H. Sasabe, J. Kido, *Org. Electron.* **2013**, *14*, **1614**.
[31] B. Domercq, R. D. Hreha, Y.-D. Zhang, N. Larribeau, J. N. Haddock, C. Schultz, S. R. Marder, B. Kippelen, *Chem. Mater.* **2003**, *15*, 1491.
[32] Y.-J. Cheng, M. S. Liu, Y. Zhang, Y. Niu, F. Huang, J.-W. Ka, H.-L. Yip, Y. Tian, A. K. Y. Jen, *Chem. Mater.* **2007**, *20*, 413.
[33] X.-C. Li, T.-M. Yong, J. Gruener, A. B. Holmes, S. C. Moratti, F. Cacialli, R. H. Friend, *Synth. Met.* **1997**, *84*, 437.
[34] A. Bacher, C. H. Erdelen, W. Paulus, H. Ringsdorf, H.-W. Schmidt, P. Schuhmacher, *Macromolecules* **1999**, *32*, 4551.
[35] M. S. Bayerl, T. Braig, O. Nuyken, D. C. Müller, M. Groß, K. Meerholz, *Macromol. Rapid Comm.* **1999**, *20*, 224.
[36] Y.-D. Zhang, R. D. Hreha, G. E. Jabbour, B. Kippelen, N. Peyghambarian, S. R. Marder, *J. Mater. Chem.* **2002**, *12*, 1703.
[37] C. D. Mueller, A. Falcou, N. Reckefuss, M. Rojahn, V. Wiederhirn, P. Rudati, H. Frohne, O. Nuyken, H. Becker, K. Meerholz, *Nature* **2003**, *421*, 829.
[38] E. Bacher, M. Bayerl, P. Rudati, N. Reckefuss, C. D. Müller, K. Meerholz, O. Nuyken, *Macromolecules* **2005**, *38*, 1640.
[39] P. Zacharias, M. C. Gather, M. Rojahn, O. Nuyken, K. Meerholz, *Angew. Chem. Inter. Ed.* **2007**, *46*, 4388.
[40] Y. Zhang, C. Zuniga, S.-J. Kim, D. Cai, S. Barlow, S. Salman, V. Coropceanu, J.-L. Brédas, B. Kippelen, S. Marder, *Chem. Mater.* **2011**, *23*, 4002.
[41] A. Charas, J. Morgado, *Curr. Phys. Chem.* **2012**, *2*, 241.
[42] G. Liaptsis, K. Meerholz, *Adv. Funct. Mater.* **2013**, *23*, 359.

© 2014 WILEY-VCH Verlag GmbH & Co. KGaA, Weinheim

[43] J. Lee, H. Han, J. Lee, S. C. Yoon, C. Lee, *J. Mater. Chem. C* **2014**, *2*, 1474.
[44] N. Rehmann, C. Ulbricht, A. Köhnen, P. Zacharias, M. C. Gather, D. Hertel, E. Holder, K. Meerholz, U. S. Schubert, *Adv. Mater.* **2008**, *20*, 129.
[45] Y.-X. Wang, M.-k. Leung, *Macromolecules* **2011**, *44*, 8771.
[46] E. Bellmann, S. E. Shaheen, S. Thayumanavan, S. Barlow, R. H. Grubbs, S. R. Marder, B. Kippelen, N. Peyghambarian, *Chem. Mater.* **1998**, *10*, 1668.
[47] S. Lee, B. Lee, B. J. Kim, J. Park, M. Yoo, W. K. Bae, K. Char, C. J. Hawker, J. Bang, J. Cho, *J. Am. Chem. Soc.* **2009**, *131*, 2579.
[48] H. J. Kim, A. R. Han, C.-H. Cho, H. Kang, H.-H. Cho, M. Y. Lee, J. M. J. Frechet, J. H. Oh, B. J. Kim, *Chem. Mater.* **2012**, *24*, 215.
[49] E. Bellmann, S. E. Shaheen, R. H. Grubbs, S. R. Marder, B. Kippelen, N. Peyghambarian, *Chem. Mater.* **1999**, *11*, 399.
[50] B. Ma, B. J. Kim, L. Deng, D. A. Poulsen, M. E. Thompson, J. M. J. Frechet, *Macromolecules* **2007**, *40*, 8156.
[51] W. Shi, S. Fan, F. Huang, W. Yang, R. Liu, Y. Cao, *J. Mater. Chem.* **2006**, *16*, 2387.
[52] H. Gao, D. A. Poulsen, B. Ma, D. A. Unruh, X. Zhao, J. E. Millstone, J. M. J. Frechet, *Nano Lett.* **2010**, *10*, 1440.
[53] D. A. Poulsen, B. J. Kim, B. Ma, C. S. Zonte, J. M. J. Frechet, *Adv. Mater.* **2010**, *22*, 77.
[54] K.-M. Yeh, C.-C. Lee, Y. Chen, *Synth. Met.* **2008**, *158*, 565.
[55] P. W. M. Blom, M. J. M. de Jong, M. G. van Munster, *Phys. Rev. B* **1997**, *55*, R656.
[56] V. D. Mihailetchi, J. K. J. van Duren, P. W. M. Blom, J. C. Hummelen, R. A. J. Janssen, J. M. Kroon, M. T. Rispens, W. J. H. Verhees, M. M. Wienk, *Adv. Funct. Mater.* **2003**, *13*, 43.
[57] V. D. Mihailetchi, H. X. Xie, B. de Boer, L. J. A. Koster, P. W. M. Blom, *Adv. Funct. Mater.* **2006**, *16*, 699.
[58] H. Kang, C.-H. Cho, H.-H. Cho, T. E. Kang, H. J. Kim, K.-H. Kim, S. C. Yoon, B. J. Kim, *ACS Appl. Mater. Interfaces* **2011**, *4*, 110.
[59] T. Earmme, E. Ahmed, S. A. Jenekhe, *J. Phys. Chem. C* **2009**, *113*, 18448.
[60] C.-N. Chuang, C.-H. Kuo, Y.-S. Cheng, C.-K. Huang, M.-k. Leung, K.-H. Hsieh, *Polymer* **2012**, *53*, 2001.
[61] T. M. Brown, J. S. Kim, R. H. Friend, F. Cacialli, R. Daik, W. J. Feast, *Appl. Phys. Lett.* **1999**, *75*, 1679.
[62] S. Guenes, H. Neugebauer, N. S. Sariciftci, *Chem. Rev.* **2007**, *107*, 1324.
[63] C. Wang, D. Hwang, Z. Yu, K. Takei, J. Park, T. Chen, B. Ma, A. Javey, *Nat. Mater.* **2013**, *12*, 899.

© 2014 WILEY-VCH Verlag GmbH & Co. KGaA, Weinheim